

# FEM Optimal Design of Wind Energy-based Heater

**Tiberiu Tudorache<sup>1</sup>, Mihail Popescu<sup>2</sup>**

<sup>1</sup>University Politehnica of Bucharest, Electrical Engineering Faculty, 313 Splaiul Independentei, Sect. 6, Bucharest, Romania, e-mail: tudorach@amotion.pub.ro

<sup>2</sup>Research Institute for Electrical Machines (ICPE - ME), 45 Tudor Vladimirescu, Bucharest, Sect. 5, Bucharest, Romania, e-mail: pd\_mihail@yahoo.com

---

*Abstract: This paper deals with the finite element based optimal design of a wind energy based heater. The proposed device ensures the conversion of the wind kinetic energy into heat by means of Joule effect of eddy currents induced in the wall of a tubular stator due to the rotating magnetic field produced by rotor permanent magnets. The transient electromagnetic field problem associated to the operation of the device is solved using a 2D finite element approach based on vector potential formulation. A simplified method for the 2D heat transfer analysis of the device is also proposed. The influence of stator wall material and thickness, number of poles, the airgap thickness and the geometrical parameters of the permanent magnets is analyzed in the aim of optimizing the studied heater.*

*Keywords: Finite element analysis, wind energy based heater, optimal design*

---

## 1 Introduction

The increasing demand of energy, the continuous reduction of existent resources of fossil fuels and the growing concern regarding the environment pollution, determined the mankind to explore new production technologies of electrical energy and heat using clean renewable sources, such as wind energy, solar energy, etc. Among the non-conventional renewable energy sources, the wind energy presents the largest potential of conversion into electric power, being able to ensure a large part of all the electrical energy need of the planet.

The conversion of wind energy into electrical energy represents one of the most promising and challenging energetic technologies, in continuous development, being cheap, clean, silent and reliable, with small maintenance costs and small ecological impact. The kinetic energy of the wind is free, practically inexhaustible, involving no polluting residues or greenhouse gases emission. The wind farms, compared to other types of electrical power plants, occupy smaller

areas and permit the connection to the existing electrical grid, ensuring the production of electrical energy at reduced costs.

The conversion principle of wind energy into electricity is not new anymore, but the design and optimization of the equipment from this class is still one of top priorities for many academic or industrial research groups all over the world. As a result of the intense research activity carried out in this area, a lot of wind turbine models were developed in many countries by several specialized companies, with rated powers ranging from some hundreds of watts up to several megawatts.

In the range of small power equipment, the wind turbines are generally used to ensure the electricity for households or for other objectives such as telecommunication devices, irrigation systems, desalination installations, battery charging systems, etc.

If we refer to the households, generally the largest part of the consumed energy is used for water heating, the other part being necessary for cooling, operation of electronic equipment, lighting, etc.

If the building heating is ensured by converting the wind energy into electricity and therefore the electricity into heating by Joule effect, the double conversion process may need inherent expensive electronic equipment. As an alternative to such systems this paper proposes a wind energy conversion system able to ensure the buildings heating by the conversion of kinetic wind energy into heat by the Joule effect of eddy currents. Studies on such innovative conversion systems are limited in number and very few references are available in the literature [1]-[4]. Such wind turbine solution could be cheaper and more reliable than the classical ones, its destination being however limited to water heating.

The topic proposed in this paper refers to the optimal design of the proposed conversion system based on a 2D finite element electromagnetic field analysis.

## **2 Operation Principle of the Wind Heater**

The operation principle of the proposed heater is based on the Joule effect of the eddy currents induced in a tubular ring due to the rotation of a magnetic field produced by one or several pairs of permanent magnets, mounted on a massive inner rotor, Fig. 1.

The massive rotor driven by the wind kinetic energy turns producing a rotating magnetic field generated by the permanent magnets. The varying magnetic field created this way leads to the development of eddy currents in the tubular stator. The water flowing through the tubular stator is heated by Joule effect, its debit being controlled by a temperature sensor in correlation with the induced power level. The electromagnetic configuration of this device is similar to a permanent magnets synchronous generator with solid conductor stator.

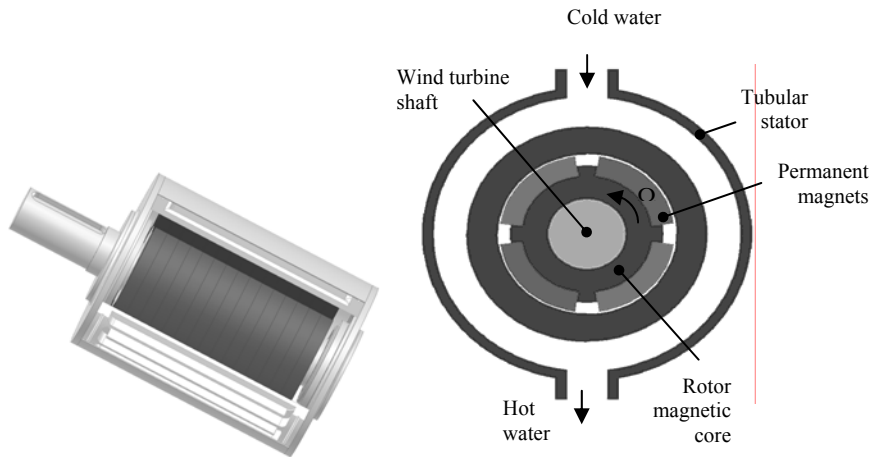


Figure 1

Principle of wind energy based heater (3D view and cross section)

The tubular stator should be thermally insulated in order to diminish the thermal losses of the device.

Such device can be used in conjunction with roof top mounted wind turbines equipped with either horizontal axis or vertical axis. In such case the distance from the household water heating system to the wind turbine is small and the thermal losses are minimal.

### 3 Electromagnetic Field Computation Model

The analysis and optimal design of the complex electromagnetic aspects associated to the proposed conversion system requires the development of robust numerical models able to simulate the device operation in various conditions, the most suitable models being those that use Finite Element Method (FEM).

The electromagnetic analysis and optimal design of the proposed device requires the solving of a transient magnetic field problem. Such analysis based on a 2D plane-parallel finite element approach can provide useful information for design engineers related to the various geometric and physical parameters that influence the induced power distribution in the stator ring such as rotor speed, airgap thickness, ring wall thickness, ring material, number of poles, etc. The proposed numerical analysis can simplify the optimization related tasks of the design engineers with the aim of maximizing the electric efficiency of the device and minimizing the materials associated costs.

The 2D electromagnetic field computation model in  $(x, y)$  cartesian coordinates is based on the magnetic vector potential formulation characterized by the partial differential equation:

$$\nabla \times \left( \frac{1}{\mu} \nabla \times \mathbf{A} - \mathbf{H}_c \right) + \sigma \left( \frac{\partial \mathbf{A}}{\partial t} - \nabla V \right) = \mathbf{0}, \quad (1)$$

where  $\mathbf{A}[0, 0, A(x, y, t)]$  is the magnetic vector potential,  $\mathbf{H}_c$  is the coercitive magnetic field,  $V$  is the electric scalar potential,  $\mu$  is the magnetic permeability and  $\sigma$  the electric conductivity. Once the magnetic vector potential chart is determined, all the derived quantities associated to the electromagnetic field such as magnetic flux density, current density etc., are easily computed.

Taking into account the physical symmetries and periodicities of the 4 pole device, Fig. 1, the electromagnetic field computation domain can be reduced to a half of a magnetic pole, Fig. 2. The two perpendicular planes (S1 and S2) delimiting a magnetic pole of the device are linked by an anticyclic type boundary condition and the inner surface of the rotor core and the outer surface of the inner stator wall (S3 and S4) are characterized by boundary conditions of tangential magnetic field type (Dirichlet  $A = 0$ ). The penetration depth of the electromagnetic field into the inner stator wall being small, the flowing water and the stator outer wall are not included into the FEM computation domain.

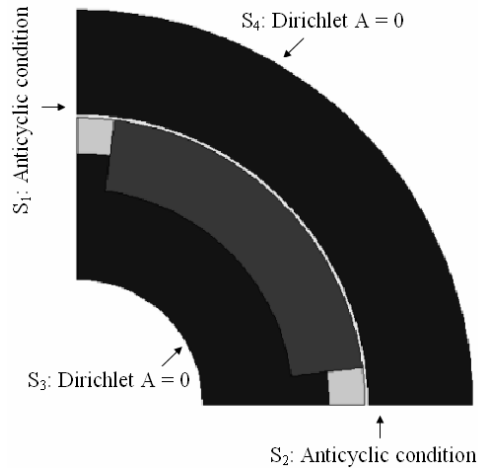


Figure 2

Computation domain and boundary conditions of 2D electromagnetic field problem  
in case of 4 pole rotor

The mesh of the computation domain, Fig. 3, is built of triangles with reduced size toward the airgap region where the most part of the magnetic energy of the conversion system is concentrated.

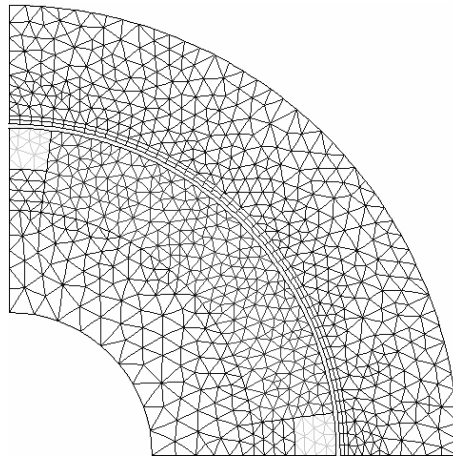


Figure 3

Finite element mesh of electromagnetic field problem in case of 4 pole rotor

The main geometric dimensions of the proposed device are as follows: shaft diameter 70 mm, length of magnets 20 mm, magnets opening angle  $75^\circ$  (magnets are made of rare earths SmCo), airgap thickness 0.5 mm, diameter of stator inner wall 222 mm, stator inner wall thickness 30 mm, diameter of rotor magnetic core 140 mm, device length in axial direction 300 mm.

## 4 Influence of Stator Wall Material on Induced Power

The material properties of the tubular stator may influence the level of induced power in the inner stator wall.

In order to evaluate this influence, successive FEM simulations were carried out for tubular stator made of aluminum, copper and steel. The numerical results presented in Fig. 4 emphasize that the induced power is the highest in case of tubular stator made of magnetic steel, material characterized by the smallest penetration depth.

A higher induced power for a given rotor speed means a higher useful power for the same level of friction and windage losses of the device and finally a higher conversion efficiency. Compared to aluminum and copper the magnetic steel used to build the tubular stator is in the same time the cheapest solution.

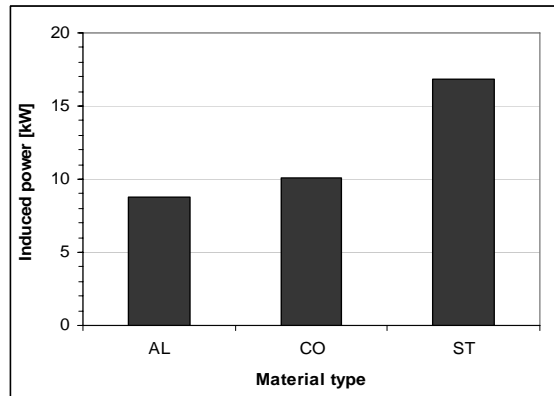


Figure 4

Induced power versus stator material

By FEM simulations carried out for a rotor speed of 400 rpm in case of a tubular stator made of steel we obtain the spectrum of magnetic field lines on the computation domain, the corresponding chart of magnetic flux density and the chart of power density induced in the inner stator wall as shown in Figs. 5-7.

Studying the results in Figs. 5-7 we can notice the deviation of magnetic field lines due to the rotor movement that generates eddy currents in the stator wall, Fig. 5, the high level of magnetic saturation in Fig. 6 and the non-uniformity of induced power density in the stator wall, Fig. 7.

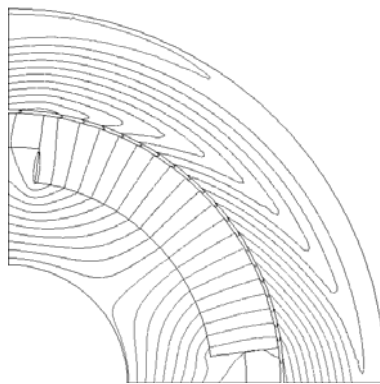


Figure 5

Magnetic field lines

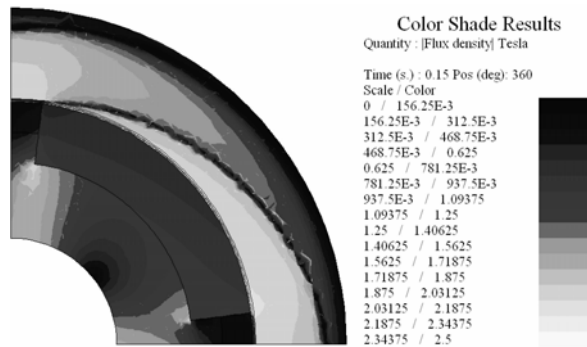


Figure 6  
Chart of magnetic flux density

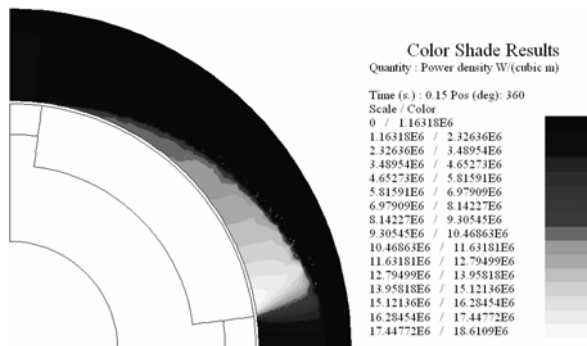


Figure 7  
Chart of induced power density in the stator inner wall

## 5 Influence of Stator Wall Material on Induced Power

The induced power in the magnetic steel made tubular stator depends on the wall thickness. In order to evaluate this dependence a FEM analysis is carried out for different values of the wall thickness between 9 mm and 49 mm.

The numerical results shown in Fig. 8, for a rotor speed of 400 rpm prove that the induced power increases strongly with the wall thickness up to an optimum value corresponding to about 30 mm, after which the increase slope becomes negligible. Thus a proper design of the studied device with minimum material costs should take into account this finding and to use magnetic steel tubes for the stator with a thickness not larger than the optimum value corresponding to the material used.

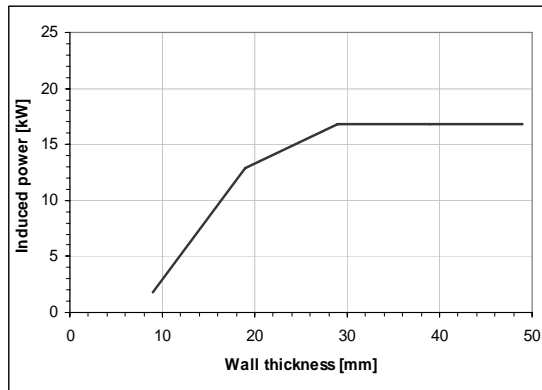


Figure 8

Induced power versus tube wall thickness

## 6 Influence of Airgap Thickness on Induced Power

Another parameter that can influence the induced power is the generator airgap thickness.

The numerical simulations carried out for various airgap values using the developed numerical 2D model prove that the induced power decrease with the increase of the airgap thickness, Fig. 9. Thus a minimum value of the airgap, limited however by the technological constraints, ensures a better electromagnetic coupling between the permanent magnets and the stator and provides a higher induced power.

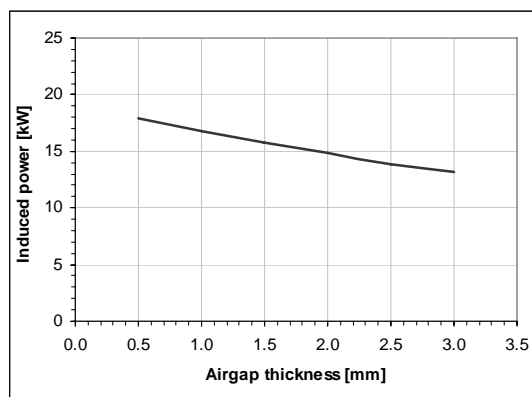


Figure 9

Induced power versus airgap thickness

## 7 Influence of Number of Poles on Induced Power

The number of poles of the generator can influence strongly the induced power value. Thus, for a given wind turbine rotor speed of 400 rpm the numerical simulations results prove that the maximum induced power is obtained for the device with 4 pole structure, Fig. 10.

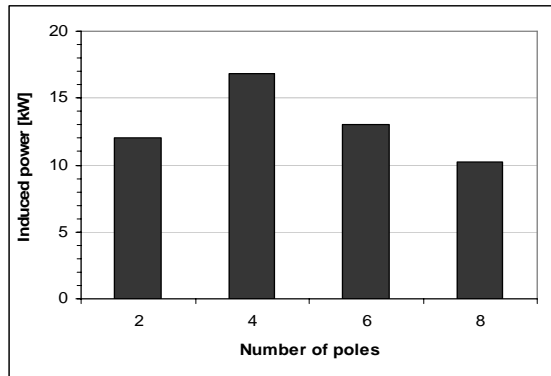


Figure 10

Induced power versus number of poles

## 8 Evaluation of Power-Speed Characteristic of the Wind Generator

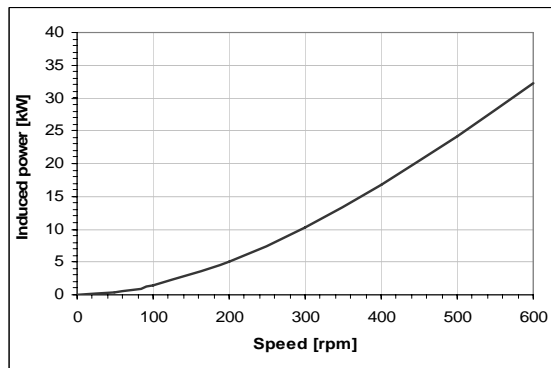


Figure 11

Induced power versus rotor speed characteristic

An important aspect related to the wind generator is the power-speed characteristic that provides information about the amount of output power of the device in various wind conditions. The numerical analysis carried out for the optimal configuration (4 pole structure, stator made of magnetic steel with inner wall thickness of 30 mm and airgap of 0.5 mm) for different wind speeds points out an induced power variation versus rotor speed as presented in Fig. 11. The profile of this curve looks like a cubic dependence between the concerned quantities.

## 9 Optimization of Device Rotor Geometry

Starting from the previously identified optimal structure of the studied heater (4 poles, stator made of magnetic steel with inner wall thickness of 30 mm and airgap of 0.5 mm) a higher induced power can be still obtained by optimizing the rotor configuration. For this purpose two geometrical parameters were used. The first one is the magnet length ML and the second parameter is the magnet opening angle MA all the geometrical data remaining unchanged. The two proposed parameters vary between imposed limits, i.e.  $ML \in [10 \text{ mm} \dots 30 \text{ mm}]$  and  $MA \in [25^\circ \dots 85^\circ]$ .

By successive FEM simulations we find for rotor speed of 400 rpm the dependence of induced power on the two geometrical parameters ML and MA as illustrated in Fig. 12.

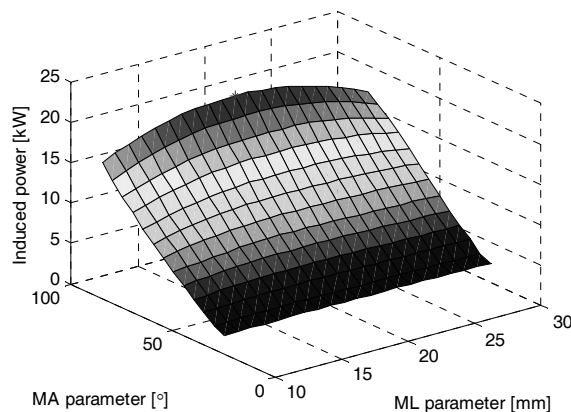


Figure 12

Induced power versus ML and MA parameters

By studying these numerical results we can notice that the maximum induced power in the stator wall is obtained for the parameters values  $ML = 20 \text{ mm}$  and  $MA = 85^\circ$ . The optimization study reveals also that for any opening angle of

permanent magnets the length of approximately 20 mm provides the highest induced power in the stator inner wall, Fig. 12.

The rotor configuration corresponding to the optimal values of the geometrical parameters ML and MA is presented in Fig. 13 along with the corresponding induced power density chart in the stator inner wall.

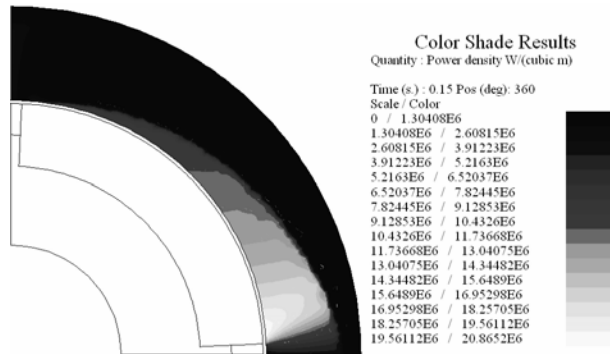


Figure 13

Chart of induced power density in the stator wall for optimal ML and MA parameters

The steady state time variation of induced power density at the point situated in the stator inner wall at 5 mm depth from the airgap surface is presented in Fig. 14. Similar variations can be obtained for any point of the stator wall.

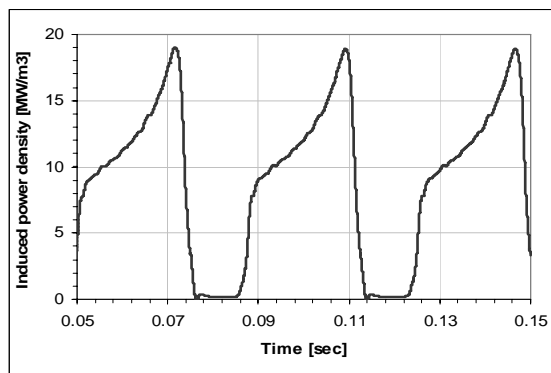


Figure 14

Time variation of induced power density in the stator inner wall in a point situated at 5 mm depth from the airgap surface for optimal ML and MA parameters

## 10 Heat Transfer Computation Model

The numerical analysis presented so far permitted us to identify the optimal structure of the proposed wind heater from electromagnetic point of view so as to maximize the induced power in the stator wall. Taking into account the fact that the optimal stator wall thickness is relatively important, i.e. 30 mm, and that the induced power level could also be important for high rotor speeds, a heat transfer analysis is necessary to estimate the temperature at the airgap level. An important temperature at the airgap level could demagnetize the permanent magnets and affect negatively the operation of the device.

The heat transfer analysis could provide useful information related to the maximum rotor speed of the wind turbine that ensures a maximum temperature of the stator inner wall smaller than 110 °C.

The heat transfer analysis is based on the steady state Fourier partial differential equation:

$$\nabla(k\nabla T) + pJ = 0, \quad (2)$$

where  $T(\mathbf{r})$  is the steady state temperature field,  $\mathbf{r}$  is the position vector of the current point,  $k = 15$  W/m/K is the thermal conductivity of steel and  $pJ$  is the thermal source represented in our case by the induced power density chart.

The thermal field computation domain is restricted to the inner stator wall heated by the Joule effect of the eddy currents, Fig. 15.

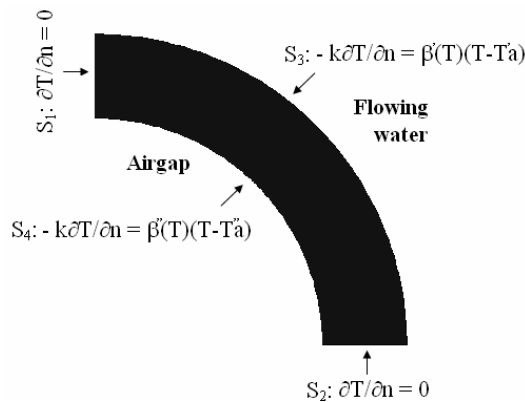


Figure 15

Computation domain and boundary conditions for the heat transfer analysis

The boundary conditions associated to the heat transfer analysis, Fig. 15, are: homogenous Neumann condition on surfaces  $S_1$  and  $S_2$  (null thermal flux) and non-homogenous Neumann conditions on surfaces  $S_3$  and  $S_4$  (thermal exchange by convection and radiation).

The temperature dependent functions of  $\beta(T)$  type in Fig. 15 take into account the convection and radiation thermal exchange as follows:

$$-k \frac{\partial \theta}{\partial n} = \sigma \varepsilon (T^4 - Ta^4) + \alpha (T - Ta) = \beta(T)(T - Ta), \quad (3)$$

where  $\sigma$  is the Stephan – Boltzmann constant,  $\varepsilon$  and  $\alpha$  are the radiation and convection thermal transfer coefficients.

The temperature  $T_a$  of the flowing water is considered 15 °C and the air temperature  $T_a$  at the airgap level is considered 20 °C, Fig. 15. The coefficients of thermal exchange by radiation on S3 and S4 are equal to 0.1 and the coefficients of thermal exchange by convection are variable in the range [1000 ... 30000] [W/m<sup>2</sup>/K] on S3 and 100 [W/m<sup>2</sup>/K] on S4. Higher convection coefficients means a higher water flow rate that is heated by the device.

The heat transfer analysis associated to the studied device is not independent from the electromagnetic one. The complete analysis of the device supposes to solve a *transient electromagnetic – transient thermal* coupling type problem. Such analysis is difficult to deal with because the electromagnetic time constant is far smaller than the thermal one. To solve such a problem means to perform at each time step associated to the electromagnetic field computation a magneto-thermal inner loop calculation that finally leads to an unreasonably huge global computation effort.

A simplified analysis method that can be considered supposes the decoupling of the electromagnetic and thermal problems. The power density  $p_J$  used in (2) is computed by an electromagnetic analysis of the device for material properties that correspond to the average temperature of the stator wall.

Based on the electromagnetic field solution the next step consists in evaluating the time average values (from time variations as in Fig. 14) of the induced power density at each point of the stator inner wall, and to use these values as a source for the heat transfer analysis. An example of time average values of the induced power density evaluation for 250 rpm is presented in Fig. 16.

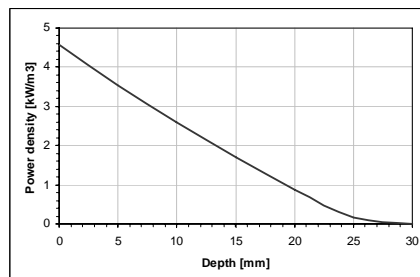


Figure 16

Time average values of induced power density in different points inside the stator inner wall as function of depth (for rotor speed of 250 rpm)

The heat transfer analysis carried out for a rotor speed of 250 rpm and a thermal transfer coefficient by convection to the flowing water  $\alpha = 1000$  [W/m<sup>2</sup>/K] reveals temperatures in the stator inner wall inferior to the imposed limit of 110 °C that can demagnetize the permanent magnets, Fig. 17.

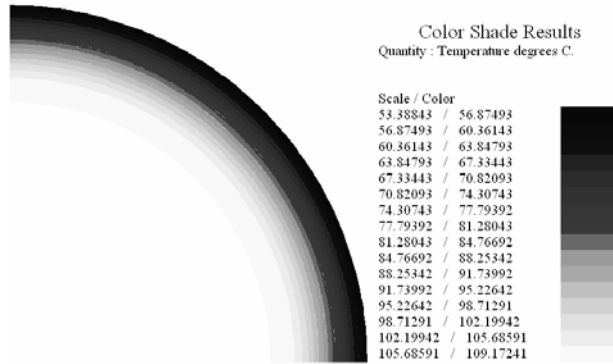


Figure 17

Temperature field on the stator inner wall for convection coefficient  $\alpha = 1000$  [W/m<sup>2</sup>/K] and rotor speed of 250 rpm

The dependence of temperature (on the inner and outer surfaces of stator wall) versus convection coefficient is presented in Fig. 18 for rotor speed of 250 rpm. Studying these results we can notice that the temperature on the inner stator surface does not increase beyond 110 °C for any considered convection coefficient. However higher rotor speeds could entail hot points with temperatures that can affect the proper operation of permanent magnets.

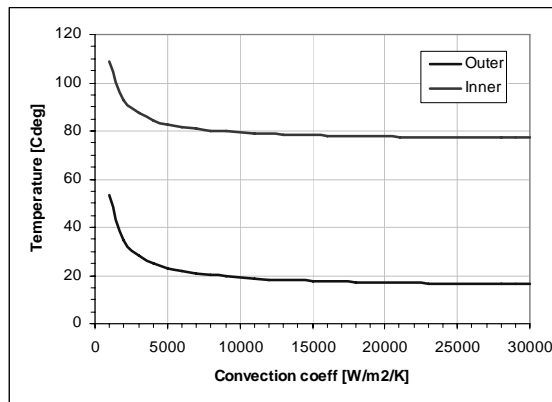


Figure 18

Temperature versus convection coefficient on the inner and outer surfaces of the stator wall at rotor speed of 250 rpm

Based on such numerical results we can afterward properly design the wind turbine blades for an optimum operation of the wind heater. Taking into account the inherent fluctuations of the wind speed an optimal operation of the proposed heater requires an efficient control system able to correlate the rotor speed and the water flow rate.

The yearly amount of energy delivered by the proposed heater depends on wind energy potential at the installation site, rotor diameter and characteristics of wind turbine, air density etc. For example to obtain 2.2 kW useful power at an average wind speed of 7 m/s a common wind turbine should have roughly a 7 m diameter rotor.

In case of series production, the manufacturing cost per power unit of a wind turbine equipped with the proposed heater is higher than the cost of solar collectors system. However a heating system based exclusively on solar collectors poses problems during the winter (exactly when the wind energy becomes more generous) when only a small amount of thermal energy can be provided. Thus a more effective solution for space and water heating is to combine the proposed wind heater with a classical system based on solar collectors. A hybrid system as proposed, could exploit both the solar and the wind energy potential that compensates naturally each other. Such solar/wind systems combination could lead to a hybrid power system with higher efficiency and reliability than in case of their separate operation.

### **Conclusions**

The numerical models of the proposed wind heater used for small power wind applications proved to be useful in the design and optimizations of the device by taking into account all the complex specific phenomena such as: magnetic saturation, skin effect in the tubular stator, space harmonics, etc.

The influence analysis was carried out with respect to various geometrical and physical parameters such as: stator material, stator wall thickness, airgap thickness, rotor geometry, rotor speed, etc.

The numerical investigation presented in the paper includes both electromagnetic and heat transfer analysis of the device.

### **Acknowledgement**

This work was supported by the Romanian Ministry of Education and Research, in the frame of the research grant PNII, 21-075/2007.

### **References**

- [1] J. Bell: Permanent Magnet Eddy Current Heat Generator, US Patent, 6011245, 2000
- [2] M. Bennetot: Device for Converting Rotational Kinetic Energy to Heat by Generating Eddy Currents, US Patent 4486638, 1984

- [3] F. Gerard: Permanent Magnet Thermal Energy System, US Patent 4511777, 1984
- [4] O. Nebi, V. Fireteanu: Analysis and Finite Element Model of a New Induction Heating Device Using Permanent Magnets, ATEE, 2008, Romania